

Lactate secreted via MCT4 from bone-colonizing breast cancer excites sensory neurons via GPR81

TATSUO OKUI¹⁻³, MASAHIRO HIASA^{3,4}, KAZUAKI HASEGAWA², TOMOYA NAKAMURA², KISHO ONO², SOICHIRO IBARAGI², TAKAHIRO KANNO¹, AKIRA SASAKI² and TOSHIYUKI YONEDA^{3,5}

¹Department of Oral and Maxillofacial Surgery, Shimane University Faculty of Medicine, Izumo, Shimane 693-8501;

²Department of Oral and Maxillofacial Surgery, Okayama University Graduate School of Medicine, Dentistry and Pharmaceutical Sciences, 2-5-1 Shikata-cho, Okayama, Okayama 700-8525, Japan; ³Department of Medicine, Hematology Oncology, Indiana University School of Medicine and The Roudebush Veterans Administration, Indianapolis, IN 46202, USA; ⁴Department of Orthodontics and Dentofacial Orthopedics, Institute of Biomedical Sciences, Tokushima University Graduate School, Tokushima, Tokushima 770-8503; ⁵Department of Cellular and Molecular Biochemistry, Osaka University Graduate School of Dentistry, Suita, Osaka 565-0871, Japan

Received July 26, 2022; Accepted December 12, 2022

DOI: 10.3892/ijo.2023.5487

Abstract. Breast cancer (BC) bone metastasis causes bone pain (BP), which detrimentally damages the quality of life and outcome of patients with BC. However, the mechanism of BC-BP is poorly understood, and effective treatments are limited. The present study demonstrated a novel mechanism of BC-BP using a mouse model of bone pain, in which mouse (EO771) and human (MDA-MB-231) BC cells were injected in the bone marrow cavity of tibiae. Western blot analysis using sensory nerves, *in vivo* assessment of cancer pain and *in vitro* calcium flux analysis were performed. These mice developed progressive BC-BP in tibiae in conjunction with an upregulation of phosphorylated pERK1/2 and cAMP-response element-binding protein (pCREB), which are molecular indicators of neuron excitation, in the dorsal root ganglia (DRG) of sensory nerves. Importantly, mice injected with BC cells, in which the expression of the lactic acid transporter monocarboxylate transporter 4 (MCT4) was silenced, exhibited decreased BC-BP with downregulated expression of pERK1/2 and pCREB in the DRG and reduced circulating levels of lactate compared with mice injected with parental BC cells. Further, silencing of the cell-surface orphan receptor for lactate, G protein-coupled receptor 81 (GPR81), in the F11 sensory neuron cells decreased lactate-promoted upregulation of pERK1/2 and Ca²⁺ influx, suggesting that the sensory neuron excitation was inhibited. These results suggested that lactate

released from BC cells via MCT4 induced BC-BP through the activation of GPR81 of sensory neurons. In conclusion, the activation of GPR81 of sensory neurons by lactate released via MCT4 from BC was demonstrated to contribute to the induction of BC-BP, and disruption of the interactions among lactate, MCT4 and GPR81 may be a novel approach to control BC-BP.

Introduction

Breast cancer (BC) frequently metastasizes to bone (1), inducing bone pain (BP) (2). BC-BP disrupts the quality of life and limits physical and mental activity of patients with BC, resulting in poor outcomes (3). Proper and satisfactory management of BP is therefore an important challenge for the improvement of quality of life and survival of these patients. The pathophysiology of BC-BP, however, remains poorly understood.

BC metastasized to bone produces increased amounts of various growth factors, cytokines and chemokines, such as TGF- β and insulin-like growth factor, that promote tumor colonization in bone and osteoclastic bone destruction, leading to the progression of bone metastasis (4,5). Of note, recent studies have shown that bone metastatic BC cells also secrete large amounts of lactic acid and protons via the plasma membrane pH regulators, including monocarboxylate transporter (MCT)1 and MCT4, carbonic anhydrases and vacuolar type ATPase (6), creating an acidic tumor microenvironment (7,8). It has been reported that under the acidic tumor microenvironment, the acid-sensing nociceptors, such as transient receptor potential vanilloid 1 and acid-sensing ion channel 3 of the sensory neurons are activated by protons, exciting sensory neurons and inducing bone pain (8-10). On the other hand, the role of lactate in the activation of sensory neurons and induction of bone pain is still unclear.

Lactate has long been considered as a waste product of cellular metabolism in anaerobic conditions. However, data

Correspondence to: Dr Tatsuo Okui, Department of Oral and Maxillofacial Surgery, Shimane University Faculty of Medicine, 89-1 Enya-cho, Izumo, Shimane 693-8501, Japan
E-mail: tokui@med.shimane-u.ac.jp

Key words: breast cancer, bone pain, lactate, monocarboxylate transporter 4, G protein-coupled receptor 81

have shown that lactate plays an important role in brain, skeletal muscle and cancer as an energy source, a gluconeogenic precursor and a signaling molecule (11). Of relevance, lactate is shown to fulfil the neuronal energy needs and provide signals to regulate neuronal functions, including excitability, plasticity and memory consolidation in the central nervous system (12). Therefore, we hypothesized that lactate also contributes to the induction of BC-BP by exciting the peripheral sensory nerves.

MCT4 is one of the key transporters involved in the regulation of intracellular translocation and extracellular secretion of lactate and protons (9) and shown to predict poor outcome in patients with triple-negative BC (13). The aim of the present study was to determine the effects of silencing MCT4 expression on the excitation of sensory neurons and induction of BC-BP. Furthermore, the role of G-protein-coupled receptor 81 (GPR81), which is recently identified as a lactate receptor (14) that regulates the neuronal network and activity (15), in the excitation of the sensory neurons was determined. The present findings demonstrated that lactate released from BC via MCT4 activates neuronal GPR81 to excite sensory neurons, leading to the induction of BC-BP.

Materials and methods

Tissue microarrays and immunohistochemical analysis. MCT4 expression in specimens of human BC and normal breast tissue was determined using tissue microarrays (cat. no. BC081116d; TissueArray.Com LLC, Rockville, MD, USA). Normal and breast cancer tissue were from different individuals. Slides were deparaffinized in xylene twice for 5 min each time, and rehydrated in 100 (twice), 95, 70 and 50% alcohol for 3 min each. Antigen retrieval was performed by heating in, 10 mM citric acid solution at 95°C for 15 min. The slides were blocked with 3% BSA (cat. no. 011-27055; FUJIFILM Wako Pure Chemical Corporation) for 30 min at room temperature. For immunohistochemical analysis, specimens were incubated with anti-MCT4 antibody (1:100; rabbit polyclonal; cat. no. sc-50329; Santa Cruz Biotechnology, Inc.) overnight at 4°C, followed by treatment with streptavidin-biotin complex (1:100; cat. no. K400311-2; EnVision System HRP-labeled polymer; Dako; Agilent Technologies, Inc.) for 60 min at room temperature and visualized with the use of a diaminobenzidine (DAB) substrate-chromogen solution (DakoCytomation Liquid DAB Substrate Chromogen System; Dako; Agilent Technologies, Inc.). Counterstaining with hematoxylin solution at room temperature for 10 sec was performed. Immunohistochemical staining positive area (%) was determined by calculating the positive area/total area ratio. Images were captured and quantification was performed using a hybrid cell count system (light microscope mode of BZ-X800 multiple analyzer BZ-H3A; Keyence Corporation) and ImageJ (Fiji) software (National Institutes of Health).

Ethics approval was not required for this research involving the use of human tissue microarray, due to the fact that this particular research fits into Section C, Paragraph 1, Part 3, Chapter 1 of Ethical Guidelines for Medical and Biological Research Involving Human Subjects issued by the Ministry of Education, Culture, Sports, Science and Technology, Japan. A waiver of ethics approval was provided by the Okayama University Ethics Committee (Okayama, Japan).

Reagents. Puromycin dihydrochloride (cat. no. sc-108071), control short hairpin (sh)RNA plasmid-A (cat. no. sc-108060), MCT4 shRNA lentivirus particles (mouse, cat. no. sc-40120-V; human, cat. no. sc-45892-V), anti-MCT4 antibody (rabbit polyclonal; cat. no. sc-50329) and anti-MCT1 antibody (mouse monoclonal; cat. no. sc-365501) were purchased from Santa Cruz Biotechnology, Inc. Anti-phosphorylated (p)-p44/42 MAPK antibody (pERK1/2; rabbit monoclonal; cat. no. 4370), anti-p44/42 MAPK antibody (ERK1/2; rabbit monoclonal; cat. no. 4695), anti-p-cAMP response element binding protein (pCREB) antibody (rabbit monoclonal; cat. no. 9198), anti-CREB antibody (rabbit monoclonal; cat. no. 9197), HRP-conjugated IgG antibody (goat anti-rabbit; cat. no. 7074), HRP-conjugated IgG antibody (goat anti-mouse; cat. no. 7076) and Alexa Fluor 488-conjugated IgG (H+L) F(ab')₂ fragment (goat anti-rabbit; cat. no. 4412) were purchased from Cell Signaling Technology, Inc. Anti-calcitonin gene-related peptide (CGRP) antibody (goat polyclonal; cat. no. ab36001) and Alexa Fluor 647-conjugated IgG H&L (donkey anti-goat; cat. no. ab150135) were purchased from Abcam. Anti-GPR81 antibody (rabbit polyclonal; cat. no. NLS2095) was purchased from Novus Biologicals, LLC. Anti-β-actin antibody (rabbit polyclonal; cat. no. ab8227) was purchased from Abcam and used as loading control.

Cell lines and culture conditions. The human BC cell lines MDA-MB-231 and MCF-7 and mouse BC cell line 4T1 were obtained from the Japanese Collection of Research Bioresources Cell Bank. Mouse BC cell line EO771 was purchased from CH3 BioSystems. Rat dorsal root ganglion (DRG) cell line F11 (a mouse N18TG2 neuroblastoma and rat DRG sensory neuron hybrid cell line) (16) has been maintained in TY's laboratory obtained from American Type Culture Collection (17). All cells were cultured in DMEM (Thermo Fisher Scientific, Inc.) supplemented with 10% heat-inactivated FBS (Biosera) and 1% penicillin-streptomycin in an atmosphere of 5% CO₂ at 37°C. All cell lines were analyzed and authenticated by targeted genomic and RNA sequencing.

Cell viability assay. BC cells were plated at 1x10⁵ cells/well (6-well plate), cultured for 48 h and the cell number was counted using a TC20 automated cell counter (Bio-Rad Laboratories, Inc.).

Determination of extracellular pH (pHe). EO771 cells (1x10⁵; 96-well plate) were cultured for 48 h in the presence of Adriamycin (cat. no. HY-15142; MedChemExpress) (30 nmol/l) to prevent cell proliferation, and pHe was measured using a FiveEasy pH meter (Mettler Toledo) immediately after cell removal from CO₂ incubator, as previously described (9).

Determination of lactate concentration. The lactate concentrations of the bone marrow fluids of tibiae, BC cell (1x10⁵) culture supernatants cultured in 12-well plates for 48 h and cell lysates of sub-confluent sh-MCT4 or sh-control EO771 cells seeded in 12-well plates for 24 h, were measured using a lactate assay kit (cat. no. ECLC-100; EnzyChrom™; BioAssay Systems) according to the manufacturer's instructions.

Intracellular Ca²⁺ mobilization. Intracellular calcium changes were determined as previously described (9). In brief, 1x10³

F11 sensory neuron cells (seeded onto 35 mm glass bottom dishes) were exposed to Fura-2AM at 3 mM (Invitrogen; Thermo Fisher Scientific, Inc.) for 15 min at room temperature. Intracellular calcium changes were monitored in a balanced salt solution (BSS) composed of NaCl 140 mM, HEPES 10 mM, glucose 10 mM, KCl 5 mM, CaCl₂ 2 mM and MgCl₂ 1 mM. Following Fura-2AM exposure, the coverslips were rinsed a total of three times in BSS.

Changes in intracellular Ca²⁺ of F11 cells after treatment with EO771 conditioned medium (CM; 30% v/v) or 10 μ M 3,5-dihydroxybenzoic acid (3,5-DHBA) (R&D Systems, Inc.) or 20 mM lactic acid (FUJIFILM Wako Pure Chemical Corporation) at room temperature were observed and recorded with digital video microfluorometry for 5 min, 90 sec and 150 sec, respectively, using an intensified CCD camera coupled to a Nikon Eclipse TE2000U microscope with Nikon Elements[®] software (Nikon Instruments Inc.). With the use of a 150 Watt xenon arc lamp, the coverslips were illuminated, and the 340/380 nm excitation wavelengths of Fura-2AM were selected by a Lambda DG-5 plus illumination system (Sutter Instrument Company). Prior to the administration of CM, 3,5-DHBA or lactic acid, sterile BSS was applied, and any cells showing a response to buffer alone were excluded from data collection.

Silencing MCT4 expression in BC cells. MDA-MB-231 and EO771 BC cells were infected with 1 μ g control shRNA (cat. no. sc-108080-V; Santa Cruz Biotechnology, Inc.) or MCT4 shRNA using a lentiviral particle transduction system (multiplicity of infection, 2.0) (cat. nos. sc-45892-V and sc-40120-V; Santa Cruz Biotechnology, Inc.) in the presence of 5 μ g/ml polybrene (sc-134220; Santa Cruz Biotechnology, Inc.) for 24 h. Subsequently, infected cells were cultured in DMEM with 10% FBS for 7 days in the presence of 2 μ g/ml puromycin to select cells stably expressing the shRNAs, following which subsequent experiments were performed. Santa Cruz Biotechnology shRNAs are provided as pools of 3 target specific 19-25 nucleotide molecules designed to knock down expression of specific genes of interest.

Silencing of GPR81 in sensory neuron cells. F11 cells were infected with 1 μ g of control shRNA or GPR81 shRNA using a lentiviral particle transduction system (multiplicity of infection, 2.0) (cat. nos. sc-108080-V and sc-44644-V; Santa Cruz Biotechnology, Inc.) in the presence of 5 μ g/ml polybrene for 24 h, and cultured in DMEM with 5% FBS for 7 days in the presence of 4 μ g/ml puromycin to select cells stably expressing the shRNAs, following which subsequent experiments were performed.

Western blot analysis. F11 cells were cultured with or without sh-control or sh-MCT4 EO771 CM (30% v/v) at 37°C for 15min. sh-GPR81 F11 cells were cultured with or without EO771 CM (30% v/v) at 37°C for 15 min. Proteins from each cell line (MDA-MB-231, EO771, MCF-7, 4T1 and F11) were obtained after lysis with RIPA lysis buffer (cat. no. 9803; Cell Signaling Technology, Inc.) and protein concentrations were measured using BCA protein assay kit (cat. no. T9300A; Takara Bio, Inc.). A total of 10 μ g of protein from the cell lysates were mixed with 4X

Laemmli sample buffer (Bio-Rad Laboratories, Inc.) and heated at 95°C for 5 min. The samples were electrophoresed using 4-12% SDS-PAGE, and the proteins were transferred onto PVDF membranes. Membranes were blocked with 5% BSA for 60 min at room temperature. The membranes were incubated with the following antibodies: Primary antibodies against MCT4 (1:1,000), pERK1/2 (1:1,000), ERK1/2 (1:1,000), CREB (1:1,000), pCREB (1:1,000) and GPR81 (1:200) were incubated overnight at 4°C. Secondary HRP-conjugated anti-rabbit (1:2,000) and HRP-conjugated anti-mouse antibodies (1:2,000) were incubated for 60 min at room temperature. An ECL reagent (cat. No. RPN2109; Amersham; Cytiva) was used to detect secondary antibody binding. A ChemiDoc MP system (Bio-Rad Laboratories, Inc.) and Image Lab software v6.1 (Bio-Rad Laboratories, Inc.) were used for the analysis of blots. β -actin (1:2,000) antibody was used as a protein loading control.

Animal model of BC-BP. All animal studies were approved by the Institutional Animal Care and Use Committee at the Indiana University School of Medicine (IACUC protocol no. 11170; Indianapolis, USA) and conducted according to the ARRIVE guidelines.

A mouse model of bone metastasis of human BC cells in 5-week-old female BALB/c athymic nude mice (n=20) and mouse BC cells in 5-week-old female C57BL/6 mice (n=20) was established (n=5/group; mean body weight, 19.5 g) (Envigo). Mice were maintained at temperature of 20°C, humidity of 50% with 12/12 h light/dark cycle and were provided with water and food *ad libitum*. Mice were injected with 1x10⁵ MDA-MB-231 human BC or EO771 mouse BC cells (parental, sh-control or sh-MCT4) using a 29-gauge needle into the bone marrow cavity of the right tibiae under anesthesia with xylazine (10 mg/kg) + ketamine (100 mg/kg) administered intraperitoneally. The sham mice received only PBS with a 29-gauge needle into the right tibial bone marrow cavity. Injection of parental, sh-control, sh-MCT4, MDA-MB-231 and EO771 cells were performed with a 29-gauge needle into the right tibial bone marrow cavity. Injection was performed by a single researcher who was blinded to the experimental conditions.

Radiological analysis of osteolytic lesions. The bone destruction in tibiae associated with MDA-MB-231 and EO771 BC tumor progression was assessed by radiography. The bones harvested at sacrifice were placed against films (22x27 cm; Fuji industrial film; FUJIFILM Wako Pure Chemical Corporation) and exposed to soft X-rays at 35 kV for 15 sec with an X-ray device (CMB-2; Softex Co., Ltd.). The area of the radiolucent osteolytic lesions was quantified using Lumina Vision/OL v2.5 analysis software (MITANI Corporation) with a light microscope (IX81; Olympus Corporation) and ImageJ software as previously described (18).

Pain behavior assay. Mice were individually placed in a cage with a glass floor, over a movable infrared light source. The light source was positioned under the center of the hind paw, and the time (sec) from stimulus onset to the paw's withdrawal was recorded. Mechanical allodynia was evaluated using von

Frey tests and a Dynamic Plantar Aesthesiometer (Ugo Basile SRL) as previously described (19). These tests are widely used for pain assessment in rodents (9). The tests were performed prior to BC cell injection to determine baseline behaviors and then every 3 days following cell injection. Throughout the experiment, behavioral tests were performed by a single researcher who was blinded to the animal experimental conditions.

At day 15 after BC cell injection, 100 μ l of blood was collected from each mouse through cardiac puncture under anesthesia with 4% isoflurane inhalation, followed by cervical dislocation. Animal death was verified by cessation of cardiovascular and respiratory movements. Ipsilateral lumbar DRGs (L3-L5) and the right tibia were then harvested for subsequent analyses. The criteria of humane endpoints for euthanasia included loss of >20% body weight compared with age-matched controls.

Harvesting of DRGs, tibiae, sera and bone marrow fluids. The collected mouse DRGs were homogenized in RIPA lysis buffer with 1 mM PMSF and phosphatase inhibitors (Na_3VO_4 and NaF). The lysate was centrifuged at 15,000 \times g for 5 min at 4°C, and the supernatant was collected as total protein. Some of the collected DRGs were fixed for 12 h at room temperature with 10% neutral-buffered formalin and then embedded in paraffin. Western blotting and immunofluorescence were subsequently performed. For the collection of bone marrow fluids from tibiae, the mouse muscles and connective tissues were removed, both ends of the tibiae were cut, and whole bone marrow was flushed out with 100 μ l PBS, followed by centrifugation (1,500 \times g; 4°C; 10 min) and collection of the supernatants.

Immunofluorescence analysis. An immunofluorescence analysis was conducted to determine the expression of pERK1/2 and CGRP, a widely used marker for sensory neurons (20), in DRGs from each group of mice using an epifluorescence microscope (BZ-X810; Keyence Corporation). Formalin-fixed paraffin-embedded tissues (as aforementioned) were sectioned with 5- μ m thickness. Slides were deparaffinized in xylene twice for 5 min each time, and rehydrated in 100 (twice), 95, 70 and 50% alcohol for 3 min each. Antigen retrieval was performed by heating in, 10 mM citric acid solution at 95°C for 5 min. The specimens were incubated with 3% BSA in PBS blocking solution for 1 h at room temperature and then with primary pERK1/2 antibody (1:200) and anti-CGRP antibody (1:200) overnight at 4°C, followed by incubation with Alexa Fluor 488 anti-rabbit IgG (1:1,000) and Alexa Fluor 647 anti-goat IgG (1:1,000) for 60 min at room temperature. Nuclei were counterstained with Fluoroshield mounting medium with DAPI (cat. no. ab104139; Abcam).

Statistical analysis. Data are presented as the mean \pm SD. The data were analyzed using an unpaired Student's t-test for comparisons between two groups or one-way ANOVA with Bonferroni's, Dunnett's or Tukey's post hoc tests for the analysis among multiple groups, using GraphPad Prism v7.0 software (GraphPad Software, Inc.). $P < 0.05$ was considered to indicate a statistically significant difference.

Results

MCT4 expression in the samples of patients with BC and BC cell lines. It was first determined whether the lactate transporter MCT4 is expressed in BC tissues compared with normal breast tissues using immunohistochemistry. Representative histological images showed that MCT4 expression in BC tissues was more intense than that in normal breast tissues (Fig. 1A). Tissue microarray analysis revealed that the MCT4-positive area of BC samples was significantly increased compared with that in normal breast tissues (Fig. 1B). These results suggested that MCT4 expression is associated with BC tumor development.

Based on these data, the expression of MCT4 and MCT1 in human (MDA-MB-231 and MCF-7) and mouse BC cell lines (4T1 and EO771) was next determined by western blot analysis, to discover human and mouse BC cell lines that exhibited high MCT4 expression and thus were suitable for further experiments. MCT1 is also the lactate transporter that controls the intra- and extracellular levels of lactate (6). Since normal breast epithelial cells are currently unavailable and the data depicted in Fig. 1A demonstrated that normal breast tissues rarely expressed MCT4, control cells were not included in the western blot analysis. EO771 BC cells showed strong expression of MCT4 and MCT1 (Fig. 1C), MDA-MB-231 cells showed moderate expression of MCT4 and MCT1, while MCT4 expression was undetectable in human MCF-7 and mouse 4T1 BC cells. Of note, these BC cells released lactate into the culture supernatant in agreement with the degree of MCT4 and MCT1 expression (Fig. 1D), demonstrating that human and mouse BC cell lines express functional MCT4.

Role of MCT4 in the excitation of sensory neurons and induction of BC-BP in mice intratibially injected with EO771 mouse BC cells. To determine the role of MCT4 in sensory neuron excitation and following BC-BP induction, MCT4 was silenced in mouse EO771 BC cells using a lentiviral system (sh-MCT4 EO771 BC cells). The expression of MCT4 protein was >80% decreased in the sh-MCT4 EO771 BC cells compared with the parental cells and sh-control cells (Fig. 2A). The expression of MCT4 in the sh-control EO771 cells did not differ from that of the parental EO771 cells. The sh-MCT4 EO771 BC cells were then injected into the bone marrow cavity of tibiae in the syngeneic female C57BL/6 mice, and the pain behavior of these mice was determined compared with the mice intratibially injected with parental or sh-control cells. No mice that received intratibial injection of mouse EO771 BC cells died until sacrifice at day 15. As previously reported using mouse 4T1 BC cells (21), the parental EO771 BC cells aggressively colonized the bone marrow cavity of tibiae accompanied with evident osteolysis (Fig. 2B, left), and sh-MCT4/EO771 BC cells also appeared to grow to an equivalent size to that of the parental EO771 BC cells in tibiae (Fig. 2B, right), suggesting that MCT4 silencing had no effects on EO771 BC growth in the bone. It is noteworthy that our previous study showed that the area of osteolysis detected on radiographs correlated well with the tumor size in bone determined by histomorphometry (18). Tumor growth could not be macroscopically observed, because the EO771 tumors grew in the bone marrow cavity. Furthermore, no

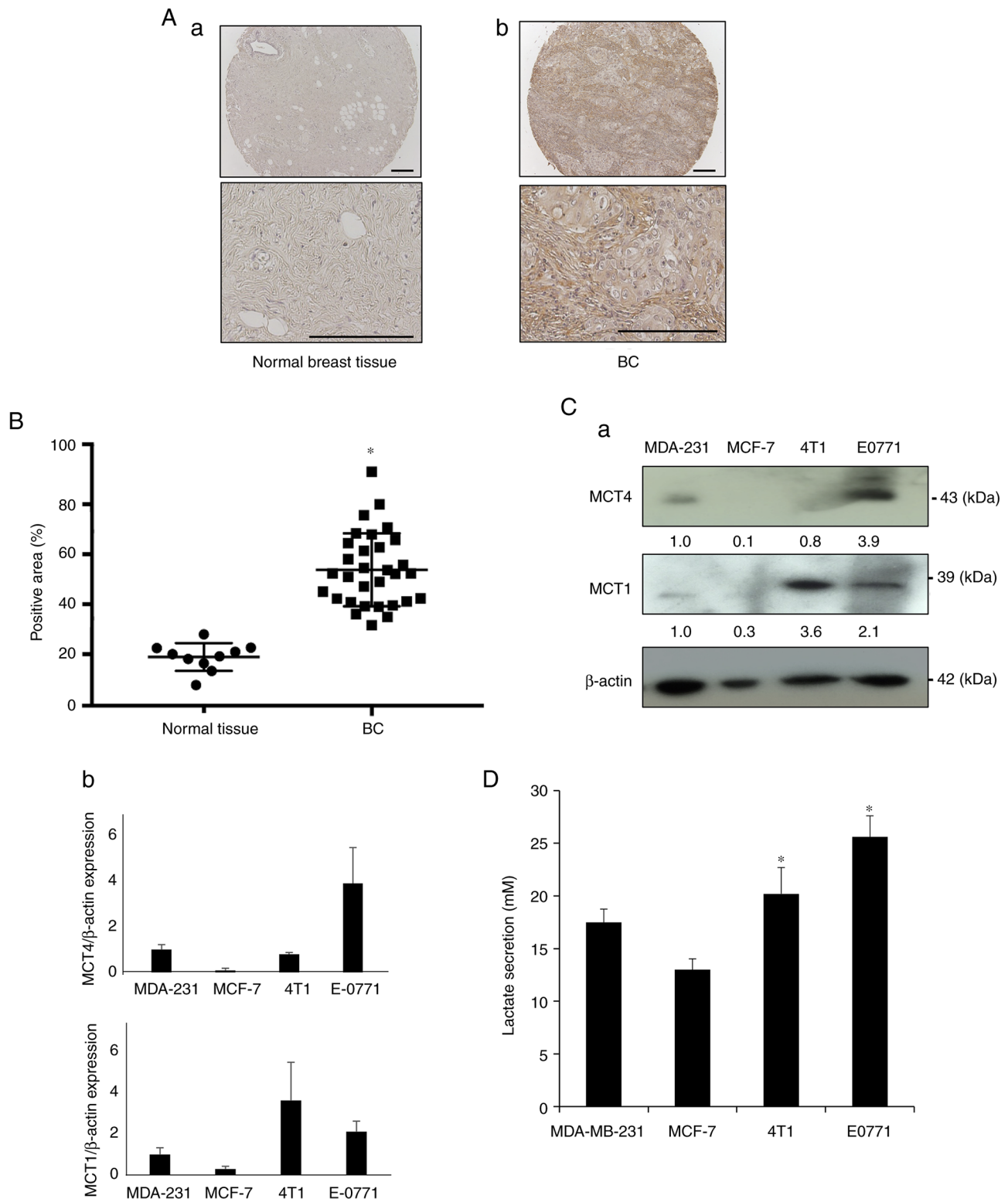


Figure 1. Expression of MCT4 in normal human breast tissues, human BC tissues and BC cell lines. (A) Immunohistochemical analysis of MCT4 expression in (a) normal breast tissue and (b) BC tissue. High power images are also shown. Scale bar, 100 μ m. (B) Scatterplot of the MCT4-positive areas in the normal human breast tissues (n=10) and human BC tissues (n=40). Immunohistochemical staining positive area (%) is shown. Data are presented as the mean \pm SD. *P<0.0001 vs. normal tissue. (C) Expression of MCT4 and MCT1 in BC cell lines (human MDA-MB-231 and MCF-7 and mouse 4T1 and E0771) analyzed by western blotting; (a) representative blot images and (b) relative ratio (MDA-MB-231 is indicated as 1.0) (n=3 per group). (D) Lactate concentration in the culture supernatants harvested from the four BC cell cultures. The lactate concentration in the culture supernatants was then determined. Data are presented as the mean \pm SD (n=4 per group). *P<0.05 vs. MCF-7. BC, breast cancer; MCT, monocarboxylate transporter.

tumor development was macroscopically detected at sites other than bone at day 15, although microscopic metastases could possibly develop in visceral organs including lung, liver

and brain (18,21). There were no differences in body weight between mice injected with the E0771 parental, sh-control and sh-MCT4 E0771 cells at day 15 (Fig. S1A).

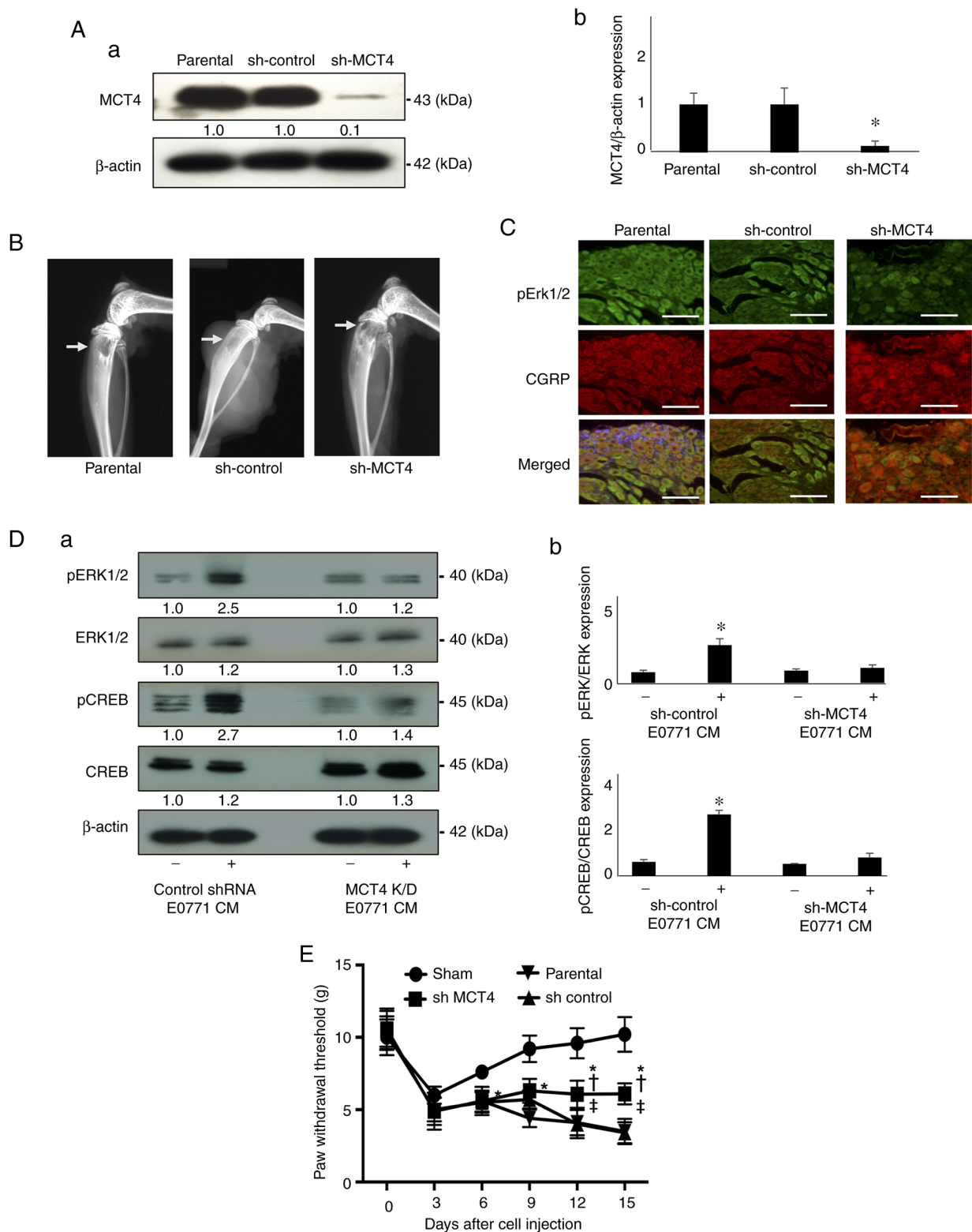


Figure 2. DRG sensory neuron excitation and mechanical allodynia determined in mice intratibially injected with E0771 mouse BC cells. (A) Expression of MCT4 in parental, sh-control and sh-MCT4 E0771 mouse BC cells examined by western analysis; (a) representative blot images and (b) relative ratio (parental is indicated as 1.0). * $P < 0.05$ vs. parental. (B) Radiograph of tumor growth showing bone destruction in the tibia of mice injected with sh-control and sh-MCT4 mouse E0771 BC cells at day 15 (arrows). (C) Expression of pErk1/2 (green, upper panel) and CGRP (red, middle panel) in DRGs harvested from mice intratibially injected with parental, sh-control and sh-MCT4 E0771 cells at day 15 by immunofluorescence. Scale bar, 50 μ m. (D) Excitation of the F11 DRG sensory neuron cells as determined by pERK1/2 and pCREB expression. The F11 DRG neuron cells were cultured in neuron basal medium in the absence or presence of conditioned medium of the sh-control and sh-MCT4 E0771 cell cultures (30%, v/v) for 15 min, lysed and the expression of pERK1/2 and pCREB was determined by western blot analysis; (a) representative blot images (control is indicated as 1.0 normalized to β -actin) and (b) relative ratio of pERK1/2 and pCREB expression (pERK1/2/ERK1/2 and pCREB/CREB) * $P < 0.05$ vs. sh-MCT4 CM. (E) Progression of the hind-paw mechanical allodynia in tibias of mice that received sham, parental, sh-control and sh-MCT4 E0771 cells ($n = 5$ per group). The pain behavior test was performed every 3 days after cell injection. Mechanical allodynia seen in all mice at day 3 is due to the surgical trauma at day 0. Data are presented as the mean \pm SD. * $P < 0.05$ vs. sham; $^{\dagger}P < 0.05$ vs. parental; $^{\ddagger}P < 0.05$ vs. sh-control. DRG, dorsal root ganglion; MCT4, monocarboxylate transporter 4; CGRP, calcitonin gene-related peptide; CREB, cAMP response element binding protein; sh, short hairpin; p, phosphorylated; CM, conditioned medium.

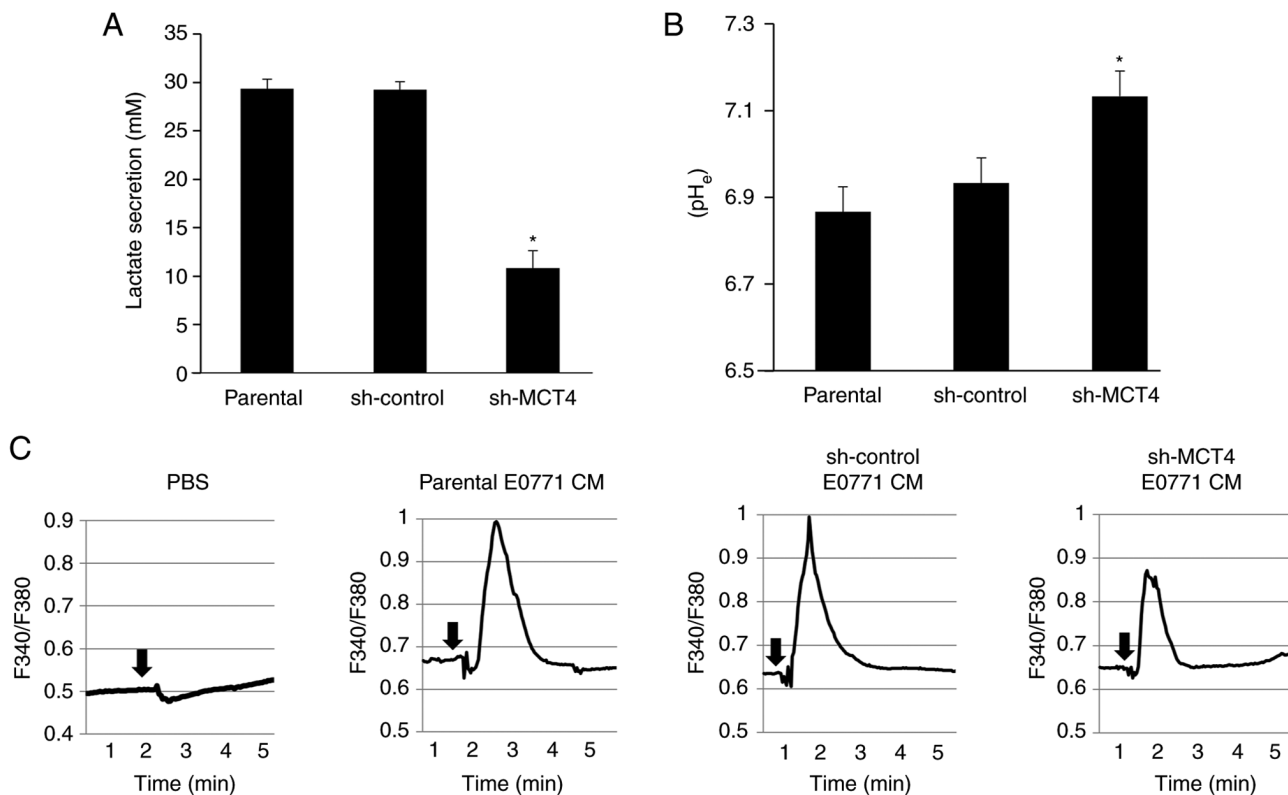


Figure 3. Role of MCT4 of EO771 mouse breast cancer cells in sensory neuron excitation. (A) Secretion of lactate by parental, sh-control and sh-MCT4 EO771 cells. Cells were cultured for 24 h, the culture supernatants were harvested, and lactate concentration was determined. Data are presented as the mean \pm SD (n=3). *P<0.01 vs. parental and sh-control. (B) pH_e of the supernatants of parental, sh-control and sh-MCT4 EO771 cells. pH_e of the same supernatants shown in A was determined. Data are presented as the mean \pm SD (n=3). *P<0.01 vs. parental and sh-control. (C) Intracellular Ca²⁺ mobilization in the F11 DRG neuron cells. MCT4, monocarboxylate transporter 4; pH_e, extracellular pH; sh, short hairpin; CM, conditioned medium.

The excitation of the DRG neurons was evaluated by immunohistochemistry using pERK1/2 as a biochemical marker for neuron excitation (17). DRGs harvested from mice injected with parental or sh-control EO771 BC cells at sacrifice (day 15) demonstrated elevated expression of pERK1/2, while the DRG of mice injected with sh-MCT4 EO771 cells showed minimum pERK1/2 expression (Fig. 2C). Interestingly, the number of the CGRP-positive sensory neurons appeared unchanged among the DRGs of the three groups of mice (Fig. 2C).

Consistent with these *in vivo* results, the F11 DRG neuron cells showed increased expression of pERK1/2 and pCREB (a biochemical marker for neuron excitation) (22) in the presence of CM (30% v/v) harvested from the cultures of the sh-control EO771 BC cells (Fig. 2D). By contrast, the expression of pERK1/2 and pCREB was not upregulated in the F11 DRG neuron cells treated with the CM of sh-MCT4 EO771 BC cells (Fig. 2D). These results supported the hypothesis that MCT4-mediated lactate release from BC leads to the excitation of the DRG sensory neurons. These *in vitro* results were also consistent with the assumption there is sufficient time and chance for the nociceptive soluble tumor products that are released as a consequence of the interactions between GPR81 at the sensory endings and cancer cells to upregulate the expression of pERK1/2 and pCREB in the DRG.

It was then determined whether MCT4 plays a role in BC-BP induction using the pain behavior assay. Mice carrying the parental or sh-control EO771 BC cells began to exhibit

decreased paw withdrawal threshold in the pain behavior assay using von Frey test at day 6 and 9 (Fig. 2E), demonstrating that these mice were developing mechanical allodynia. Mechanical allodynia advanced as a function of time in parallel with EO771 BC growth in the bone. By contrast, mice intratibially injected with sh-MCT4 EO771 BC cells showed reduced mechanical allodynia compared with mice carrying parental or sh-control EO771 BC cells (Fig. 2E). These results suggested that MCT4 plays an important role in BC-BP induction by mediating lactate release. Lactate acidosis may also contribute to the induction of BC-BP represented by mechanical allodynia by activating acid-sensing nociceptors, such as the transient receptor potential vanilloid 1 and acid-sensing ion channels (23).

Role of MCT4 expression in EO771 mouse BC cells. The effects of MCT4 knockdown on lactate metabolism in EO771 mouse BC cells were subsequently investigated *in vitro*. Lactate secretion into the culture supernatants was significantly decreased (Fig. 3A) and pH_e was significantly elevated (Fig. 3B) in sh-MCT4 EO771 cells compared with those in the parental and sh-control EO771 cells. These results suggested that MCT4 regulates lactate secretion and pH_e in EO771 mouse BC cells.

In addition, the CM of parental and sh-control EO771 BC cell cultures also increased Ca²⁺ influx, a widely used indicator of sensory neuron excitation (24), in the F11 DRG neuron cells, while sh-MCT4 EO771 CM increased Ca²⁺ influx to a lesser

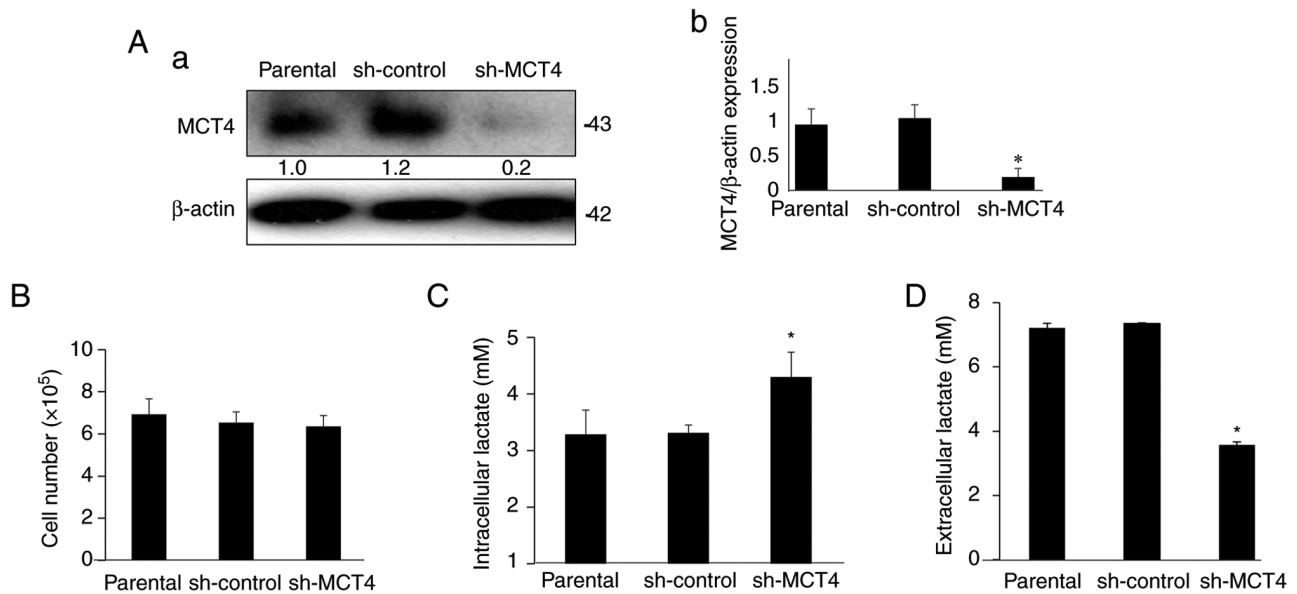


Figure 4. Role of MCT4 in lactate metabolism in MDA-MB-231 human BC cells. (A) MCT4 expression in parental, sh-control and sh-MCT4 MDA-MB-231 human BC cells analyzed by western blotting; (a) representative blot images and (b) relative ratio (parental is indicated as 1.0). * $P < 0.01$ vs. parental and sh-control ($n = 3$). (B) Cell viability of parental, sh-control and sh-MCT4 MDA-MB-231 human BC cells. Cells were cultured for 48 h and the cell number was counted. There was no significant difference in the numbers of cells. Data are presented as the mean \pm SD ($n = 3$). (C) Intracellular levels of lactate in parental, sh-control and sh-MCT4 MDA-MB-231 human BC cells. Data are presented as the mean \pm SD ($n = 3$). * $P < 0.01$ vs. parental and sh-control ($n = 3$). (D) Extracellular levels of lactate in parental, sh-control and sh-MCT4 MDA-MB-231 human BC cells. Data are presented as the mean \pm SD ($n = 3$). * $P < 0.01$ vs. parental and sh-control ($n = 3$). BC, breast cancer; MCT4, monocarboxylate transporter 4; sh, short hairpin.

extent than the CM of parental and sh-control EO771 BC cells (Fig. 3C). Consistent with the present results, the F11 cells are reported to display functional DRG neuron properties, including unique neuronal morphology of extended neurites and Ca^{2+} mobilization in response to stimuli (25) without the presence of glia cells. Furthermore, it was recently found that the F11 cells possess neuron-like properties, responding to the soluble products released from BC cells (data not shown). These data will be investigated in future studies. Taken together, these results suggested that lactate released from EO771 mouse BC cells via MCT4 excites sensory neuron cells.

Role of MCT4 expression in lactate metabolism and BP induction in MDA-MB-231 human BC cells. The role of MCT4 expression in lactate metabolism and BP induction in human MDA-MB-231 BC cells was next investigated. To this end, MCT4 was knocked down in MDA-MB-231 cells by introducing shRNA plasmids using a lentiviral system, thereby generating sh-MCT4 MDA-MB-231 cells. The expression of MCT4 protein was $>80\%$ decreased in the sh-MCT4 MDA-MB-231 cells compared with the parental cells and sh-control cells (Fig. 4A). The expression of MCT4 in the sh-control MDA-MB-231 cells did not differ from that of the parental MDA-MB-231 cells.

Cell proliferation was not changed among parental, sh-control and sh-MCT4 MDA-MB-231 cells (Fig. 4B). Importantly, the intracellular lactate level was increased (Fig. 4C) and lactate secretion was reduced by $\sim 40\%$ (Fig. 4D) in sh-MCT4 MDA-MB-231 cells compared with those in the parental and sh-control MDA-MB-231 cells. These results suggested that MCT4 regulates intracellular and extracellular levels of lactate in human MDA-MB-231 BC cells.

Role of MCT4 expression in lactate levels in bone marrow and BC-BP induction. Subsequently, the role of MCT4 in BC-BP after intratibial injection of MDA-MB-231 cells in Balb/c athymic nude mice was determined. Mice injected with MDA-MB-231 sh-control and sh-MCT4 cells showed bone destruction associated with tumor growth on the radiographs at day 7 (Fig. 5A). There was no significant difference in the extent of bone destruction between the MDA-MB-231 sh-control and sh-MCT4-injected mice (Fig. 5A and B).

To examine the effects of MCT4 expression on BC-BP induction in mice, a mechanical allodynia test was performed at day 10. Mice intratibially injected with parental and sh-control MDA-MB-231 BC cells exhibited mechanical allodynia (Fig. 5C). By contrast, mechanical allodynia was significantly decreased in mice injected with sh-MCT4 MDA-MB-231 cells compared with mice injected with parental and sh-control MDA-MB-231 BC cells (Fig. 5C), suggesting that MCT4 expression is critical to BC-BP induction.

The lactate concentration in the bone marrow fluid of tibiae injected with MDA-MB-231 human BC cells was also determined. Lactate concentration was elevated in the fluids harvested from the bone marrow of tibiae injected with sh-control MDA-MB-231 BC cells compared with that of sham-operated tibiae (Fig. 5D). By contrast, lactate concentration in the fluids harvested from the bone marrow of tibiae injected with sh-MCT4 MDA-MB-231 cells was not significantly increased compared with those injected with sh-control MDA-MB-231 cells (Fig. 5D). These results collectively suggested that inhibition of MCT4 expression decreased lactate release from BC cells into the bone marrow cavity, which in turn reduced BC-BP. There were no differences in body weight between mice injected with the MDA-MB-231

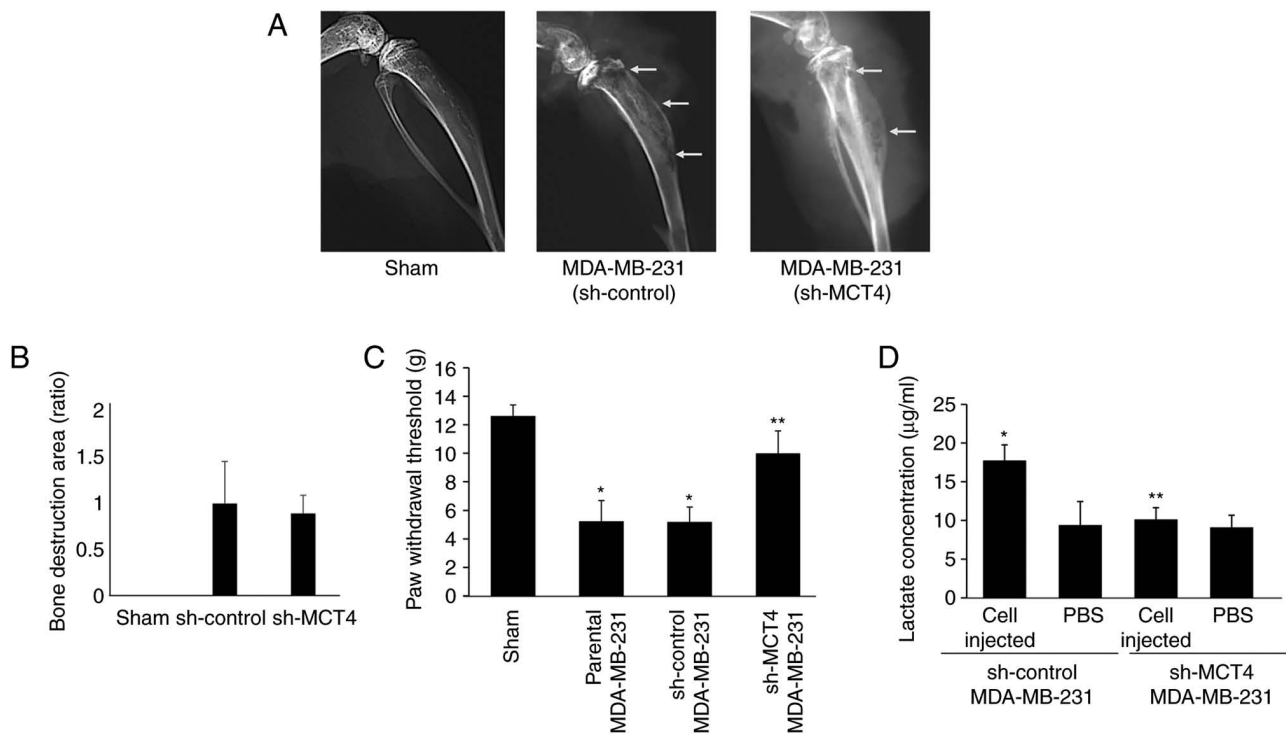


Figure 5. Role of MCT4 in BC-BP induction in mice intratibially injected with MDA-MB-231 human BC cells. (A) Radiograph of tumor growth showing bone destruction in the tibia (arrows) of mice injected with the MDA-MB-231 sh-control and sh-MCT4 human BC cells at day 7 after cell injection. (B) Quantitative analysis of the area of bone destruction seen in A. Data are presented as the mean \pm SD (n=5). (C) Hind-paw mechanical allodynia in tibiae of mice intratibially injected with parental, sh-control and sh-MCT4 MDA-MB-231 human BC cells. The behavior test was performed at day 7. Data are presented as the mean \pm SD (n=5). *P<0.05 vs. sham and **P<0.05 vs. parental and sh-control. (D) Lactate concentrations in the bone marrow fluids harvested from tibiae injected with sh-control or sh-MCT4 MDA-MB-231 BC cells or PBS. Data are presented as the mean \pm SD (n=4). *P<0.05 vs. PBS and **P<0.05 vs. sh-control. BC, breast cancer; BP, bone pain; MCT4, monocarboxylate transporter 4; sh, short hairpin.

parental, sh-control and sh-MCT4 MDA-MB-231 cells at day 15 (Fig. S1B).

Role of the lactate receptor GPR81 in sensory neuron excitation. Finally, the mechanism via which BC-secreted lactate excites the sensory neurons to induce BC-BP was determined. GPR81 has been initially found as a lactate receptor that mediates lipolysis in the adipose tissue (14). It has been also shown that GPR81 regulates neuronal network activity in cooperation with other GPRs (26). However, little is known about the expression and function of GPR81 in sensory neurons. The present study found that F11 DRG neuron cells express GPR81 by western blot analysis (Fig. 6A). To determine the role of GPR81 in sensory neuron excitation, GPR81-knockdown F11 DRG neuron cells were established via shRNA transduction (sh-GPR81 F11 cells). GPR81 protein expression was reduced by 70% in sh-GPR81 F11 DRG neuron cells compared with parental and sh-control F11 cells (Fig. 6A). Of note, the CM harvested from EO771 BC cultures, which contains high levels of lactate, increased the expression of pERK1/2 in the F11 cells (Fig. 6B), which was almost abolished in the sh-GPR81 F11 cells. These results suggested that GPR81 contributes to sensory neuron excitation caused by BC-derived lactate.

Consistent with these results, treatment with the GPR81 agonist 3,5-DHBA (27) increased Ca^{2+} influx in parental and sh-control F11 cells (Fig. 6C), which was not observed in sh-GPR81 F11 cells (Fig. 6C). Furthermore, lactic acid

treatment also increased Ca^{2+} influx in parental F11 cells (Fig. 6D), which was reduced in sh-GPR81 F11 cells. These results provided additional evidence supporting that GPR81 plays important roles in the excitation of sensory neurons by lactate.

Discussion

Cancer cells produce large amounts of lactate resulting from the Warburg effect (28) and actively secrete it via the lactate transporter MCT4 (13) to avoid cell death due to intracellular lactate acidosis. Secreted lactate is then taken up by neighboring cells, such as stromal, endothelial and immune cells, in the tumor microenvironment via the lactate transporter MCT1 as an energy source (29). Interestingly, stromal cells in turn release lactate via MCT4, which is then incorporated by cancer cells via MCT1 as an energy source for ATP generation (known as reverse Warburg effect) (30). However, the effects of lactate released via MCT4 from cancer on the sensory neurons innervating the tumor microenvironment are poorly understood. The present study showed that human BC tissues express increased MCT4 compared with normal breast tissues, suggesting that MCT4 is associated with BC development. Furthermore, it was found that mouse and human BC cell lines also substantially express MCT4 to increase lactate secretion, thereby lowering pH_e, and in turn decrease intracellular lactate levels. Consistent with these *in vitro* results, lactate levels in the bone marrow fluids of

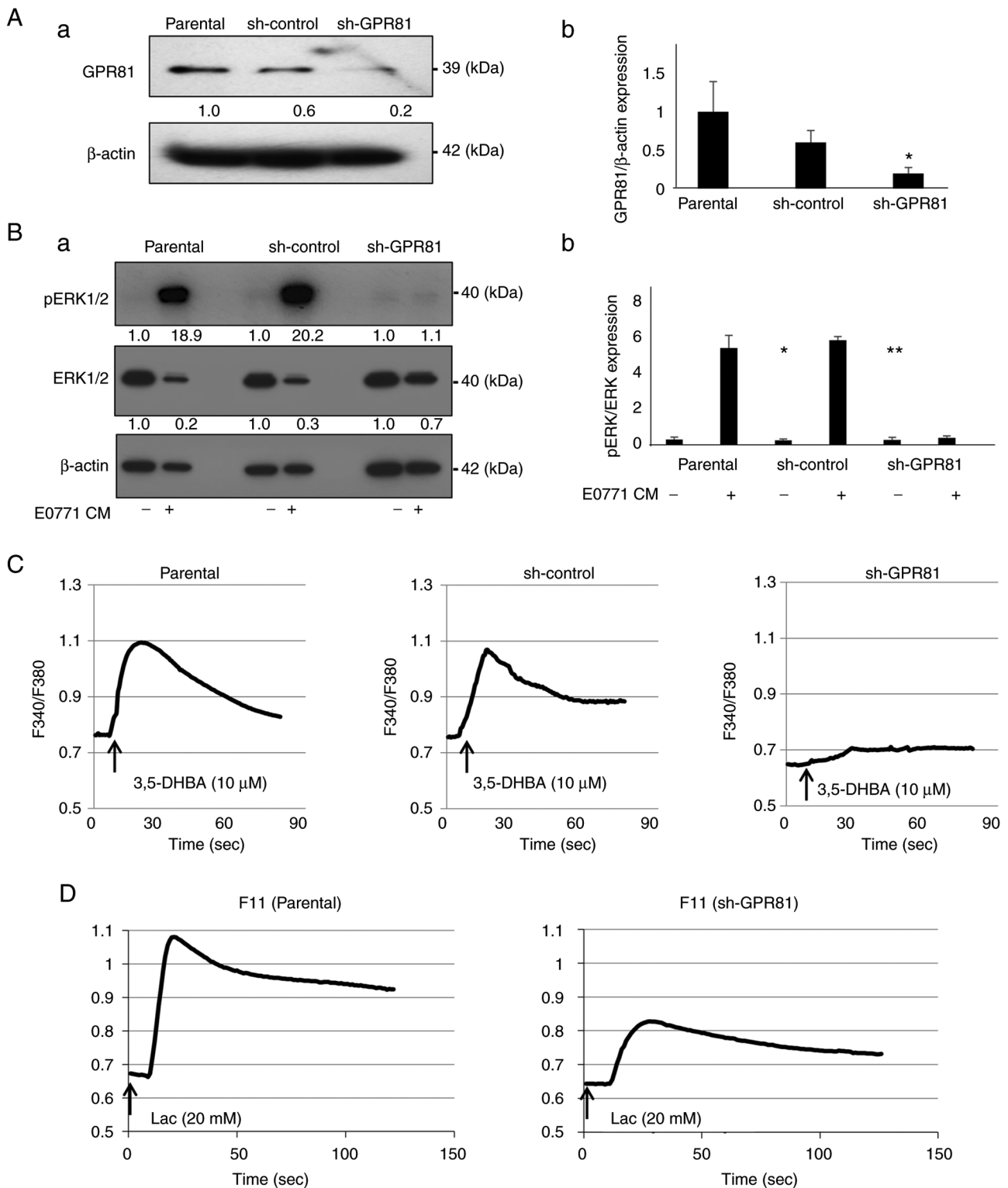


Figure 6. Role of the lactate receptor GPR81 in the excitation of the F11 DRG sensory neuron cells. (A) Expression of GPR81 in the parental, sh-control and sh-GPR81 F11 DRG cells analyzed by western blotting; (a) representative blot images and (b) relative ratio (parental is indicated as 1.0) ($n=3$). (B) pERK1/2 expression in the F11 DRG sensory neuron cells. Cells were treated with or without E0771 CM (30%, v/v) for 15 min, lysed and the expression of pERK1/2 was analyzed by western blotting; (a) representative blot images (control is indicated as 1.0 normalized to β-actin) and (b) relative ratio of pERK1/2 expression (pERK1/2/ERK1/2). * $P<0.01$ vs. parental CM (-); ** $P<0.01$ vs. sh-control CM (-) ($n=3$). (C) Intracellular Ca^{2+} mobilization in the F11 DRG sensory neuron cells treated with or without the GPR81 agonist 3,5-DHBA ($n=10$). (D) Intracellular Ca^{2+} mobilization in the F11 DRG sensory neuron cells treated with or without lactic acid ($n=10$). GPR81, G-protein-coupled receptor 81; 3,5-DHBA, 3,5-dihydroxybenzoic acid; sh, short hairpin, CM, conditioned medium; DRG, dorsal root ganglion.

tibiae in mice injected with MDA-MB-231 human BC cells were elevated. Importantly, these effects were all inhibited

when MCT4 expression was knocked down in BC cells. In addition, it was also demonstrated that intratibial injection of

EO771 mouse BC cells and MDA-MB-231 human BC cells in mice caused sensory nerve excitation and BC-BP induction, which was attenuated after intratibial injection of EO771 BC cells with MCT4 is knockdown. Taken together, these results demonstrated that the supply of lactate by BC to the sensory nerves via MCT4 in the tumor microenvironment causes the excitation of sensory nerves, which consequently induces BC-BP. The present results suggested that MCT4 of BC is an important player in the excitation of the sensory neurons and induction of BC-BP. Blocking MCT4 actions may thus be an effective novel approach for the treatment of BC-BP.

It should be noted that active secretion of excess intracellular lactate facilitates the development of an acidic tumor microenvironment, which has been shown to promote cancer progression by increasing tumor angiogenesis, proteolytic activity, metastatic potential and resistance to immune system and anticancer therapies (31). Furthermore, increased MCT4 expression is associated with poor outcome in patients with triple-negative BC (32). It has also been reported that MCT4 expression is increased in head and neck cancer (28). Hence, the present results provide additional pieces of evidence that MCT4-mediated active lactate excretion is associated with BC progression, suggesting that MCT4 may also be a potential therapeutic target for BC treatment (33).

The present study demonstrated that sensory neurons express GPR81 that mediates the effects of BC-derived lactate to excite sensory neurons. The current results showed that lactate, as a signaling molecule, bound to and activated its cognitive receptor GPR81 to excite sensory neurons leading to the upregulation of pERK1/2 expression. However, the downstream signaling pathways that are propagated following lactate binding to GPR81 were not determined in the present study. It has been reported that GPR81 regulates neuronal network activity in cooperation with other GPRs (26). Identification of GPR81 signaling pathways involving ERK1/2 and CREB in association with sensory neuron excitation and BC-BP induction is important to design pharmacological interventions for BC-BP.

The results of the present study that GPR81 plays a role in the promotion of the excitation of sensory neurons are not consistent with previous results reporting that GPR81 activation inhibits neuron excitation (15,34). The reasons for this discrepancy are unknown. The present results could be due to an involvement of certain indirect routes. Along this line, it has been reported that GPR81 modulates the expression of MCT1 and MCT4, which are responsible for the regulation of cellular lactate metabolism by controlling lactate uptake and release (35,36). It is therefore speculated that MCT1/MCT4 affects GPR81 role in neurons. Determination of the interactions between GPR81 and MCT1/MCT4 in the regulation of neuronal activity is important to define the effects of GPR81 on neurons.

The present study showed that lactate released from BC via the lactate transporter MCT4 changes sensory neuron excitation and BC-BP induction, presumably following the binding to the lactate receptor GPR81 of the DRG neurons, indicating that cancer regulates neuronal activity in a paracrine manner. Of interest, recent studies reported that neuronal activity in turn modulates cancer progression and metastasis (37-39). Various types of cancer have been reported to exhibit

increased expression of GPR81, which is associated with their progression (35,40). In agreement with these reports, BC tissue of patients showed elevated GPR81 expression compared with normal human breast tissue by immunohistochemistry, and knockdown of GPR81 decreased BC growth in subcutis and bone in mice (36). Taken together, these results suggested that GPR81 plays a role not only in neuron excitation by lactate released from BC via MCT4 in a paracrine manner but also promotion of cancer progression by BC-derived lactate in an autocrine manner. It is intriguing to determine the effects of the activation or suppression of GPR81 of DRG neurons on cancer aggressiveness.

There are several limitations in the present study. Firstly, the present study did not provide compelling evidence that GPR81 plays a pivotal role in the pathophysiology of BC-BP. Using von Frey test, which has long and widely been used in pain behavior assays, it was shown that mice intratibially injected with EO771 BC cells displayed mechanical allodynia, suggesting that these mice developed BC-BP. However, the present study did not demonstrate data of spinal sensitization maintained as a consequence of lactate activation of GPR81 on the C-nociceptors, which is a prerequisite for mechanical allodynia. Secondly, the present study did not present some critical data, including the expression of GPR81 on the peripheral ending and DRG C-nociceptors, the effects of GPR81 on pain behaviors of GPR81^{-/-} mice intratibially injected with BC cells compared with wild-type mice and the effects of GPR81 antagonists on pain behaviors of these mice. These studies are currently ongoing. Thirdly, it has been previously demonstrated that the area of bone destruction detected on radiographs corresponds well with the tumor size in bone determined by histomorphometry (21); however, the present study lacks histomorphometric data of EO771 BC tumor size in bone. Fourthly, the present results may raise the question whether the tumor growth in bone is correlated with the degree of lactate production and/or MCT4 expression. This point was not specifically determined in the present study, although it appeared that no such correlation existed. It has been demonstrated that tumor growth is modulated not only by tumor activity but also surrounding microenvironments (41). The effects of the tumor microenvironments may mask the effects of lactate/MCT4 on tumor growth. Finally, since the cell line data had no adequate normal control, these data should be cautiously interpreted.

In conclusion, the current findings suggested that lactate transported via MCT4 from BC excites sensory neurons through binding and activating GPR81 of the sensory neurons. Unraveling the GPR81 signaling pathways in sensory neurons should increase the understanding of the mechanism of lactate regulation of BC-BP and facilitate the design of mechanism-based therapies for the control of BC-BP, for which effective treatments are currently limited.

Acknowledgements

Not applicable.

Funding

The present work was supported by a Grant-in-Aid for Research Activity and Grant-in-Aid for Young Scientists

from JSPS KAKENHI to TO from the Ministry of Education, Culture, Sports, Science and Technology of Japan (grant nos. 16H0699219 and 18K1722500), a Grant-in-Aid for Scientific Research from JSPS KAKENHI to TY (grant no. 17H04377) and the IU Health Strategic Research Initiative in Oncology to TY (grant no. 46-875-54) and start-up fund of the Indiana University School of Medicine to TY (grant no. 2382696 YONED).

Availability of data and materials

The datasets used and/or analyzed during the current study are available from the corresponding author on reasonable request.

Authors' contributions

TO and TY conceived and designed the experiments. TO, MH, KH, TN and KO performed the experiments. TO and TY analyzed and interpreted the data. TO, MH, KH, TN, KO, SI, TK and AS performed data acquisition. TO and TY wrote the paper. TO, TY, MH, KH, TN, KO, AS, TK and SI performed manuscript revision/review. TO, MH and TY confirm the authenticity of all the raw data. All authors read and approved the final manuscript.

Ethics approval and consent to participate

All animal studies were approved by the Institutional Animal Care and Use Committee at the Indiana University School of Medicine (IACUC protocol no. 11170; Indianapolis, USA) and conducted according to the ARRIVE guidelines.

Patient consent for publication

Not applicable.

Competing interests

The authors declare that they have no competing interests.

References

- Clézardin P, Coleman R, Puppo M, Ottewill P, Bonnelye E, Paycha F, Confavreux CB and Holen I: Bone metastasis: Mechanisms, therapies, and biomarkers. *Physiol Rev* 101: 797-855, 2021.
- Falk S and Dickenson AH: Pain and nociception: Mechanisms of cancer-induced bone pain. *J Clin Oncol* 32: 1647-1654, 2014.
- Qiao RQ, Zhang HR, Ma RX, Li RF and Hu YC: Prognostic factors for bone survival and functional outcomes in patients with breast cancer spine metastases. *Technol Cancer Res Treat* 21: 15330338221122642, 2022.
- Hu W, Zhang L, Dong Y, Tian Z, Chen Y and Dong S: Tumour dormancy in inflammatory microenvironment: A promising therapeutic strategy for cancer-related bone metastasis. *Cell Mol Life Sci* 77: 5149-5169, 2020.
- Infante M, Fabi A, Cognetti F, Gorini S, Caprio M and Fabbri A: RANKL/RANK/OPG system beyond bone remodeling: Involvement in breast cancer and clinical perspectives. *J Exp Clin Cancer Res* 38: 12, 2019.
- Ngo DC, Ververis K, Tortorella SM and Karagiannis TC: Introduction to the molecular basis of cancer metabolism and the Warburg effect. *Mol Biol Rep* 42: 819-823, 2015.
- Tiedemann K, Hussein O and Komarova SV: Role of altered metabolic microenvironment in osteolytic metastasis. *Front Cell Dev Biol* 8: 435, 2020.
- Avnet S, Di Pompo G, Lemma S and Baldini N: Cause and effect of microenvironmental acidosis on bone metastases. *Cancer Metastasis Rev* 38: 133-147, 2019.
- Hiasa M, Okui T, Allette YM, Ripsch MS, Sun-Wada GH, Wakabayashi H, Roodman GD, White FA and Yoneda T: Bone pain induced by multiple myeloma is reduced by targeting V-ATPase and ASIC3. *Cancer Res* 77: 1283-1295, 2017.
- Yoneda T, Hiasa M, Nagata Y, Okui T and White FA: Acidic microenvironment and bone pain in cancer-colonized bone. *Bonekey Rep* 4: 690, 2015.
- Brooks GA: The science and translation of lactate shuttle theory. *Cell Metab* 27: 757-785, 2018.
- Magistretti PJ and Allaman I: Lactate in the brain: From metabolic end-product to signalling molecule. *Nat Rev Neurosci* 19: 235-249, 2018.
- Payen VL, Mina E, Van Hée VF, Porporato PE and Sonveaux P: Monocarboxylate transporters in cancer. *Mol Metab* 33: 48-66, 2020.
- Cai TQ, Ren N, Jin L, Cheng K, Kash S, Chen R, Wright SD, Taggart AK and Waters MG: Role of GPR81 in lactate-mediated reduction of adipose lipolysis. *Biochem Biophys Res Commun* 377: 987-991, 2008.
- de Castro Abrantes H, Briquet M, Schmuziger C, Restivo L, Puyal J, Rosenberg N, Rocher AB, Offermanns S and Chatton JY: The Lactate Receptor HCAR1 Modulates neuronal network activity through the activation of G_{α} and $G_{\beta\gamma}$ Subunits. *J Neurosci* 39: 4422-4433, 2019.
- Francel PC, Harris K, Smith M, Fishman MC, Dawson G and Miller RJ: Neurochemical characteristics of a novel dorsal root ganglion X neuroblastoma hybrid cell line, F-11. *J Neurochem* 48: 1624-1631, 1987.
- Nakanishi M, Hata K, Nagayama T, Sakurai T, Nishisho T, Wakabayashi H, Hiraga T, Ebisu S and Yoneda T: Acid activation of Trpv1 leads to an up-regulation of calcitonin gene-related peptide expression in dorsal root ganglion neurons via the CaMK-CREB cascade: A potential mechanism of inflammatory pain. *Mol Biol Cell* 21: 2568-2577, 2010.
- Okui T, Shimo T, Fukazawa T, Kurio N, Hassan NM, Honami T, Takaoka M, Naomoto Y and Sasaki A: Antitumor effect of temsirolimus against oral squamous cell carcinoma associated with bone destruction. *Mol Cancer Ther* 9: 2960-2969, 2010.
- Okui T, Hiasa M, Ryumon S, Ono K, Kunisada Y, Ibaragi S, Sasaki A, Roodman GD, White FA and Yoneda T: The HMGB1/RAGE axis induces bone pain associated with colonization of 4T1 mouse breast cancer in bone. *J Bone Oncol* 26: 100330, 2021.
- Russell FA, King R, Smillie SJ, Kodji X and Brain SD: Calcitonin gene-related peptide: Physiology and pathophysiology. *Physiol Rev* 94: 1099-1142, 2014.
- Hiraga T, Myoui A, Hashimoto N, Sasaki A, Hata K, Morita Y, Yoshikawa H, Rosen CJ, Mundy GR and Yoneda T: Bone-derived IGF mediates crosstalk between bone and breast cancer cells in bony metastases. *Cancer Res* 72: 4238-4249, 2012.
- Kawasaki Y, Kohno T, Zhuang ZY, Brenner GJ, Wang H, Van Der Meer C, Befort K, Woolf CJ and Ji RR: Ionotropic and metabotropic receptors, protein kinase A, protein kinase C, and Src contribute to C-fiber-induced ERK activation and cAMP response element-binding protein phosphorylation in dorsal horn neurons, leading to central sensitization. *J Neurosci* 24: 8310-8321, 2004.
- Leffler A, Mönter B and Koltzenburg M: The role of the capsaicin receptor TRPV1 and acid-sensing ion channels (ASICs) in proton sensitivity of subpopulations of primary nociceptive neurons in rats and mice. *Neuroscience* 139: 699-709, 2006.
- Ouyang K, Zheng H, Qin X, Zhang C, Yang D, Wang X, Wu C, Zhou Z and Cheng H: Ca^{2+} sparks and secretion in dorsal root ganglion neurons. *Proc Natl Acad Sci USA* 102: 12259-12264, 2005.
- Pastori V, D'Aloia A, Blasa S and Lecchi M: Serum-deprived differentiated neuroblastoma F-11 cells express functional dorsal root ganglion neuron properties. *PeerJ* 7: e7951, 2019.
- Lauritzen KH, Morland C, Puchades M, Holm-Hansen S, Hagelin EM, Lauritzen F, Attramadal H, Storm-Mathisen J, Gjerdde A and Bergersen LH: Lactate receptor sites link neurotransmission, neurovascular coupling, and brain energy metabolism. *Cereb Cortex* 24: 2784-2795, 2014.
- Liu C, Kuei C, Zhu J, Yu J, Zhang L, Shih A, Mirzadegan T, Shelton J, Sutton S, Connelly MA, *et al.*: 3,5-Dihydroxybenzoic acid, a specific agonist for hydroxycarboxylic acid 1, inhibits lipolysis in adipocytes. *J Pharmacol Exp Ther* 341: 794-801, 2012.

28. Hasegawa K, Okui T, Shimo T, Ibaragi S, Kawai H, Ryumon S, Kishimoto K, Okusha Y, Monsur Hassan NM and Sasaki A: Lactate transporter monocarboxylate transporter 4 induces bone pain in head and neck squamous cell carcinoma. *Int J Mol Sci* 19: 3317, 2018.
29. Doherty JR and Cleveland JL: Targeting lactate metabolism for cancer therapeutics. *J Clin Invest* 123: 3685-3692, 2013.
30. Liang L, Li W, Li X, Jin X, Liao Q, Li Y and Zhou Y: 'Reverse Warburg effect' of cancer-associated fibroblasts (Review). *Int J Oncol* 60: 67, 2022.
31. Corbet C and Feron O: Tumour acidosis: From the passenger to the driver's seat. *Nat Rev Cancer* 17: 577-593, 2017.
32. Doyen J, Trastour C, Ettore F, Peyrottes I, Toussant N, Gal J, Ilc K, Roux D, Parks SK, Ferrero JM and Pouyssegur J: Expression of the hypoxia-inducible monocarboxylate transporter MCT4 is increased in triple negative breast cancer and correlates independently with clinical outcome. *Biochem Biophys Res Commun* 451: 54-61, 2014.
33. Hong CS, Graham NA, Gu W, Espindola Camacho C, Mah V, Maresh EL, Alavi M, Bagryanova L, Krotee PAL, Gardner BK, *et al*: MCT1 modulates cancer cell pyruvate export and growth of tumors that Co-express MCT1 and MCT4. *Cell Rep* 14: 1590-1601, 2016.
34. Ordenes P, Villar PS, Tarifeño-Saldivia E, Salgado M, Elizondo-Vega R, Araneda RC and García-Robles MA: Lactate activates hypothalamic POMC neurons by intercellular signaling. *Sci Rep* 11: 21644, 2021.
35. Roland CL, Arumugam T, Deng D, Liu SH, Philip B, Gomez S, Burns WR, Ramachandran V, Wang H, Cruz-Monserrate Z and Logsdon CD: Cell surface lactate receptor GPR81 is crucial for cancer cell survival. *Cancer Res* 74: 5301-5310, 2014.
36. Ishihara S, Hata K, Hirose K, Okui T, Toyosawa S, Uzawa N, Nishimura R and Yoneda T: The lactate sensor GPR81 regulates glycolysis and tumor growth of breast cancer. *Sci Rep* 12: 6261, 2022.
37. Venkatesh HS: The neural regulation of cancer. *Science* 366: 965, 2019.
38. Zahalka AH and Frenette PS: Nerves in cancer. *Nat Rev Cancer* 20: 143-157, 2020.
39. Silverman DA, Martinez VK, Dougherty PM, Myers JN, Calin GA and Amit M: Cancer-associated neurogenesis and nerve-cancer cross-talk. *Cancer Res* 81: 1431-1440, 2021.
40. Brown TP, Bhattacharjee P, Ramachandran S, Sivaprakasam S, Ristic B, Sikder MOF and Ganapathy V: The lactate receptor GPR81 promotes breast cancer growth via a paracrine mechanism involving antigen-presenting cells in the tumor microenvironment. *Oncogene* 39: 3292-3304, 2020.
41. Hanahan D and Weinberg RA: Hallmarks of cancer: The next generation. *Cell* 144: 646-674, 2011.



This work is licensed under a Creative Commons Attribution-NonCommercial-NoDerivatives 4.0 International (CC BY-NC-ND 4.0) License.